Small Angle X-Ray Scattering

What information can you get from this technique?

Small Angle X-Ray Scattering

<u>A wide range of fields:</u>

Medicine
Biology
Chemistry
Physics
Archaeology
Environmental and conservation sciences
Materials

<u>A wide range of systems:</u>

Polymer processing
Self assembly of mesoscopic metal particles
Colloids
Inorganic aggregates
Liquid crystals
The supramolecular organisation in biological systems
The structure and function of muscle filaments
Corneal transparency

Size range comparisons

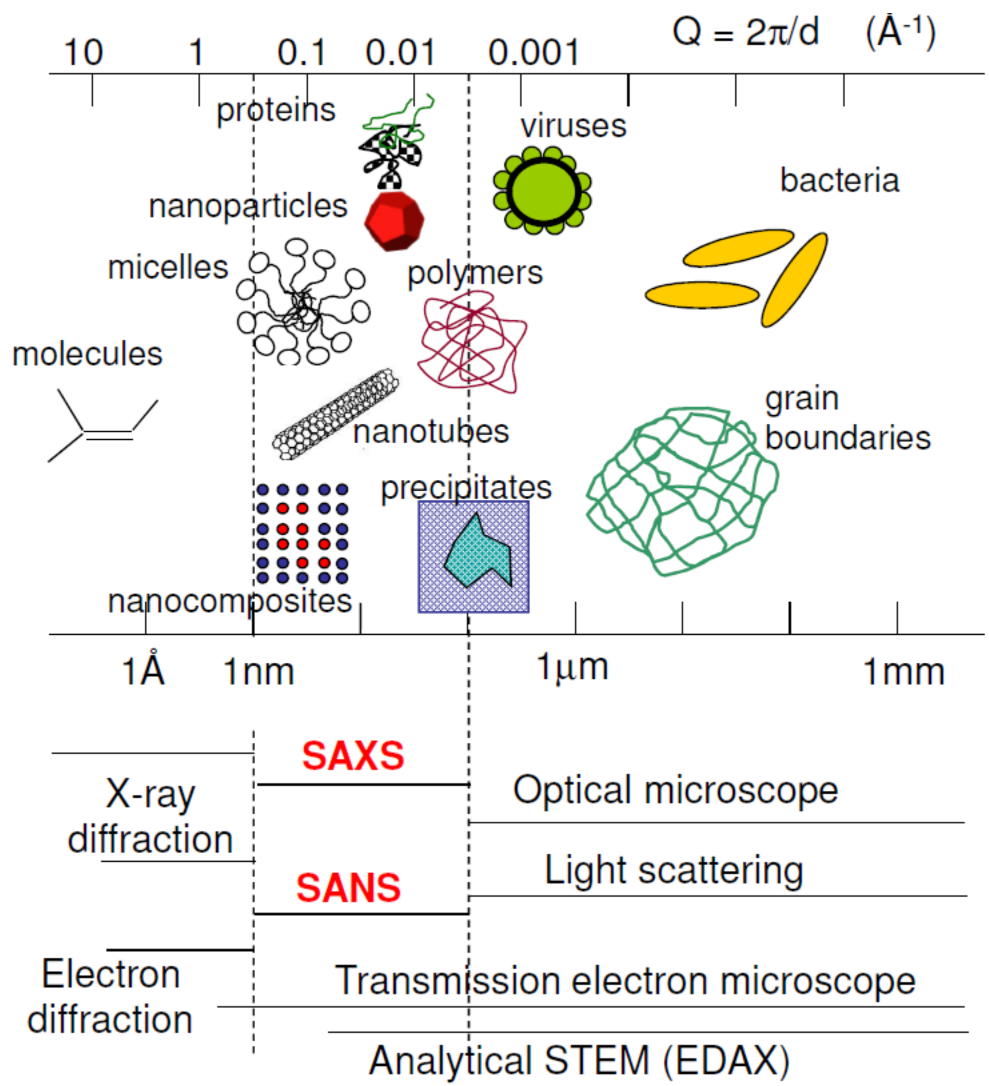

Beamline specifications

Wavelength (Energy) range	0.9 - 1.9 Å (6.5 -13 keV)
Flux at sample	>1.25 10^{11} ph/s 1.24 Å for a beam current of 250 mA
Bandpass (ΔE/E)	< 10^{-4}
Beam size at sample	Variable between ~65 - 1200 µm horizontally ~30 - 265 µm vertically
Beam divergence at sample	<0.5x0.1 $mrad^2$
Q range SAXS	0.0066-0.7 $Å^{-1}$
2Θ range WAXS	3.0° - 62°

Sample environments

- Thermo-stated liquid cell (Required volume on demand)
- Non thermo-stated liquid cell rack for 24 samples (Volume 30ml)
- Thermo-stated ladder for 6 capillaries (1mm or 2mm diameter)
- Non thermo-stated ladder for 20 capillaries (1mm diameter)
- One film holder for 45 samples
- 1 Linkam stage for 1mm capillaries
- 1 Linkam stage for 22mm diameter films

	Controller	Pumping system	Linkam Stage	
Sample type			Capillary	Film
Model	T95	LNP954	HFSX350-CAP	THMS600
Max Temp (ºC)	1500	-196	350	600
Max rate (ºC/min)	200	100	30	150

Experimental considerations

Thickness of the sample

- Affect transmission
- Affect the shape of the curve (Difficult to analyse)

Aim to 70% transmission

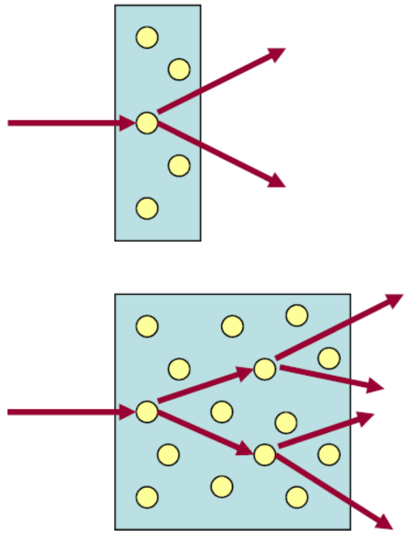

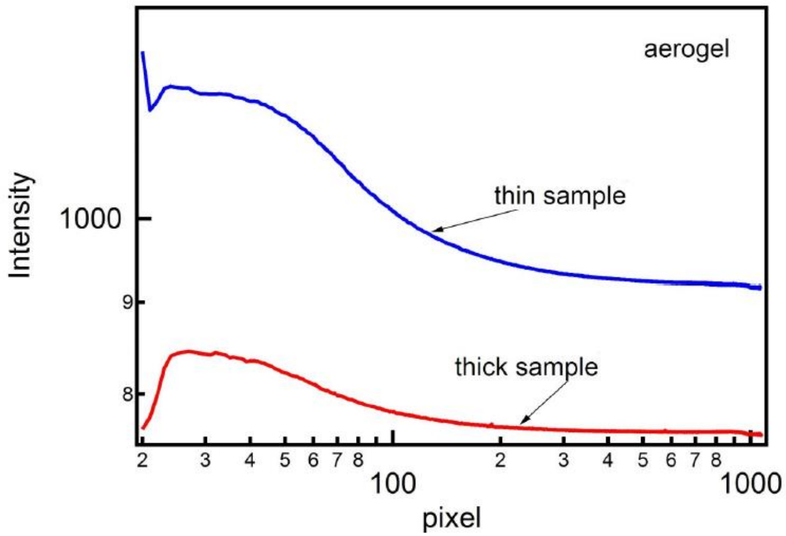

Experimental considerations

Thickness of the sample

The maximum scattering intensity is achieved by selecting the optimal thickness of the sample.
The scattering intensity can be formulated as:

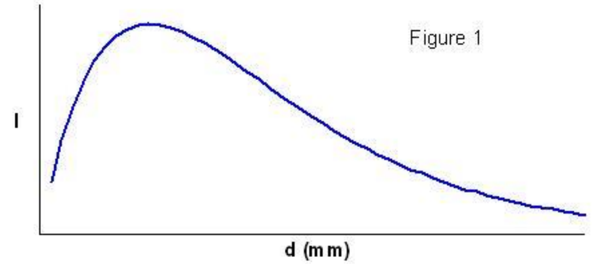

d: the thickness of the sample

μ: linear absorption coefficient

Optimal thickness $$\frac{\partial I}{\partial d} = k(1-\mu d)e^{-\mu d} \Rightarrow d_{optimal} = \frac{1}{\mu}$$

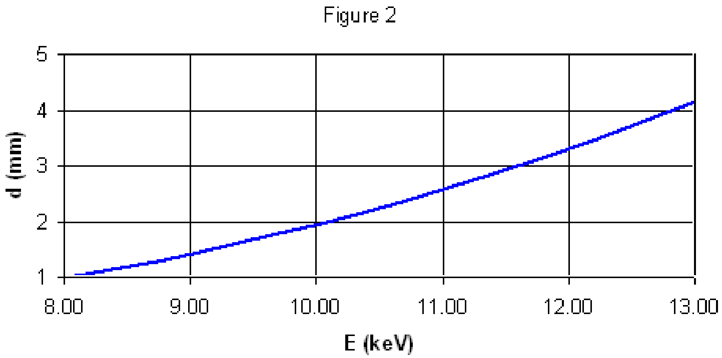

The linear absorption coefficient can be calculated or measured.
Optimal thickness of the sample (water in this case) as a function of the energy.

Experimental considerations

Concentration

Big particle scatter more
Higher concentration

better signal **But don't burn out the detector**
can complicate analysis

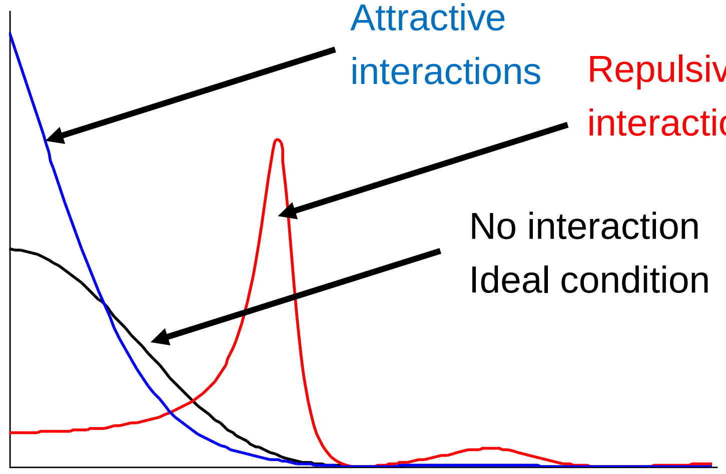

Minimum concentration for synchrotron: ≈ 1mg/ml

Experimental considerations

High concentration
Interaction between particles

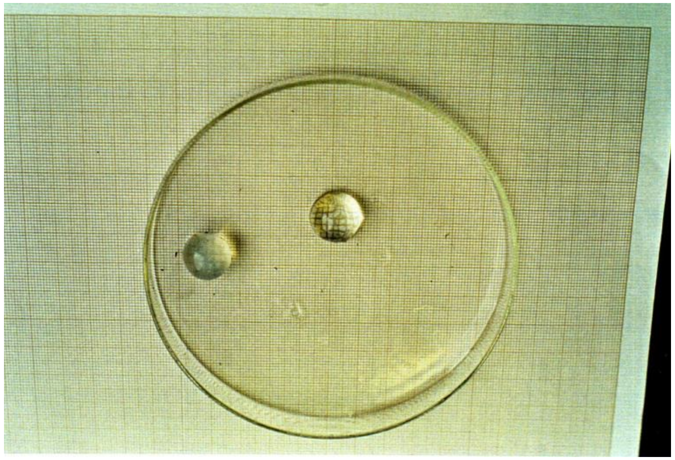

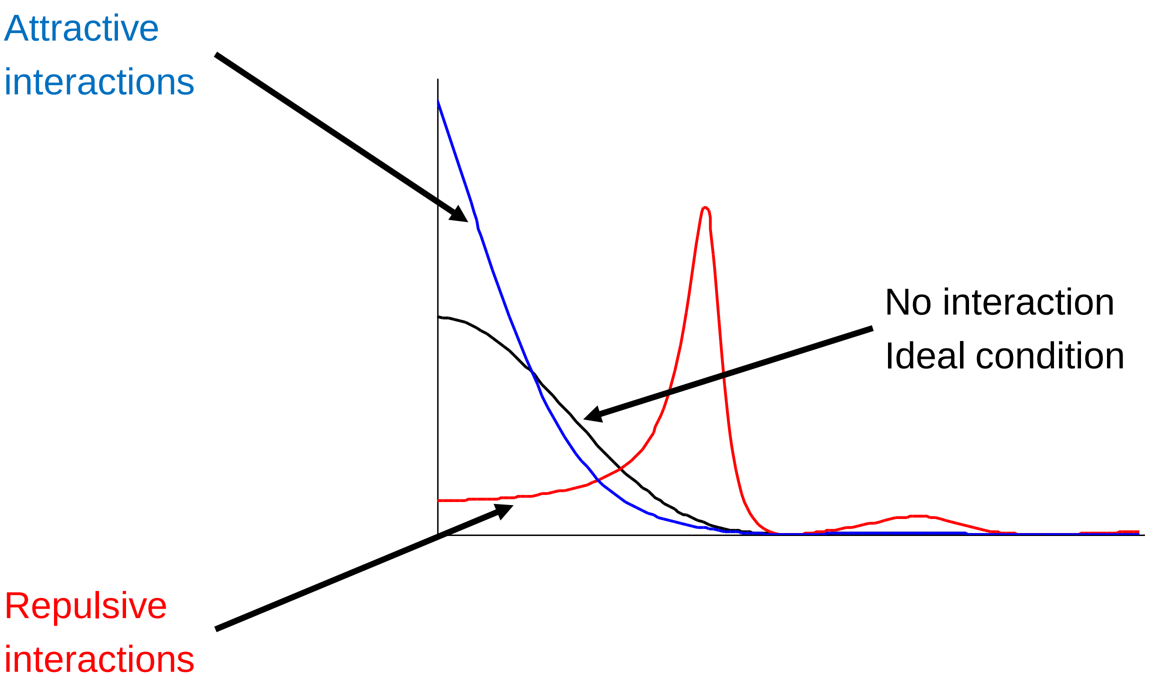

Experimental considerations

Contrast

When the monster came, Lola, like the peppered moth remained motionless and undetected. Harold, of course, was immediately devoured.

The electronic density of the particle MUST not match the electronic density of the matrix.

Experimental setup

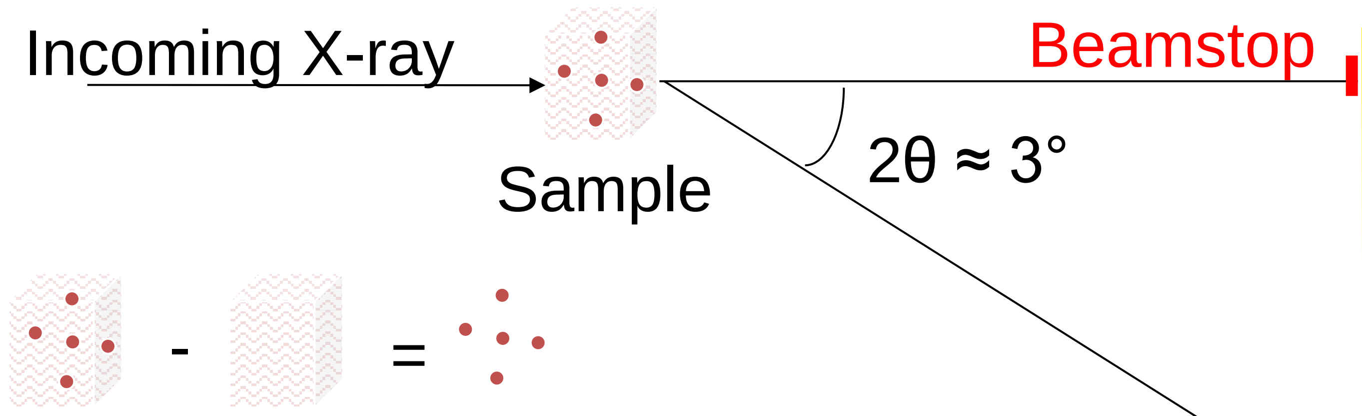

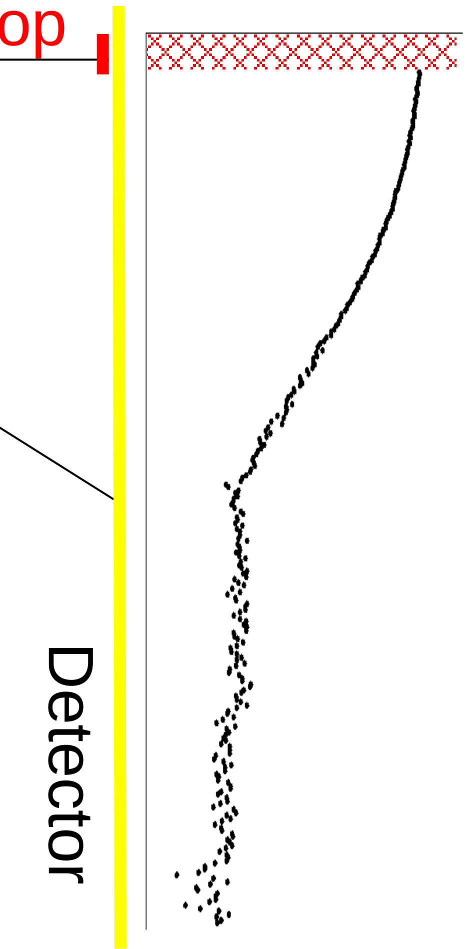

We want to know the scattering intensity from the sample of interest (e.g. proteins)

We have to subtract the background

Empty cell + matrix

Fibre – 1 –

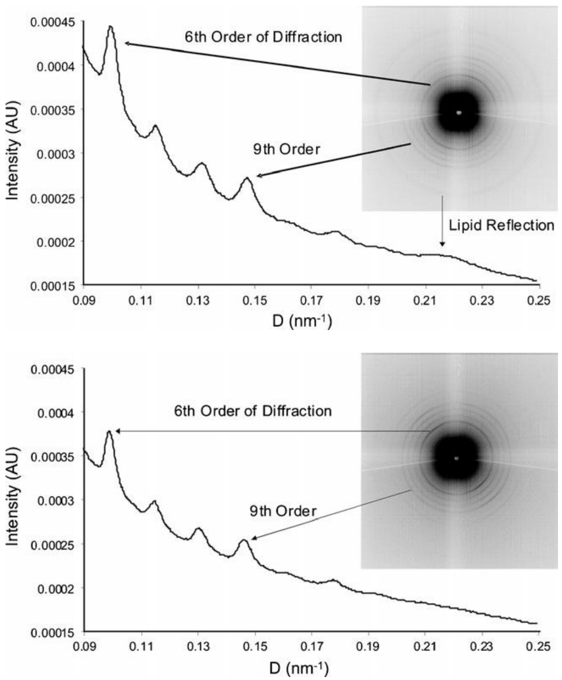

After 1 h of extraction, the 0.22 nm^{-1} reflection is still observed However, after 4 h of extraction, the 0.22 nm^{-1} reflection no longer appears, indicating that the lipid phase of the parchment sample has been removed

Lipids decreases shrinkage temperature.

Parchment more degraded at the corner of the page by manual handling

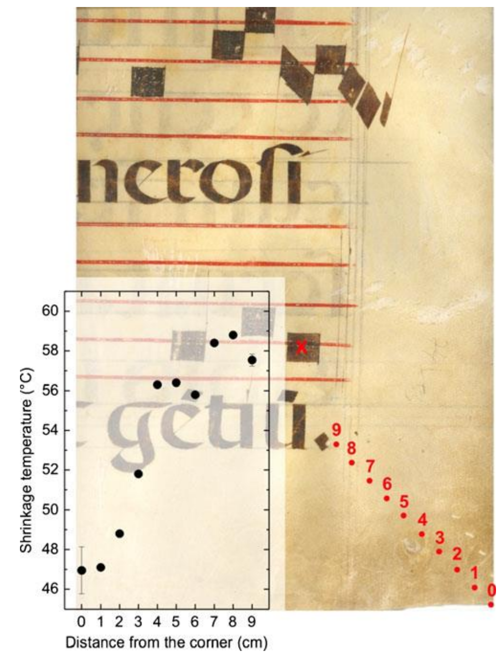

Možir *et al.*, A study of degradation of historic parchment using small-angle X-ray scattering, synchrotron-IR and multivariate data analysis, Anal Bioanal Chem (2012) 402:1559–1566 DOI 10.1007/s00216-011-5392-6

Fibre – 2 –

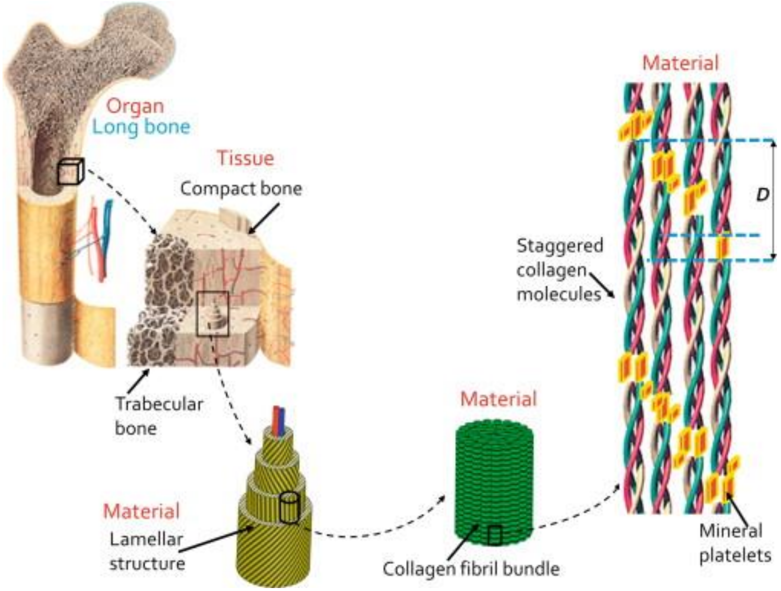

Strain, stress, and other mechanical parameters determination at small scales (< 100 nm) in nanostructured biomineralized composites.

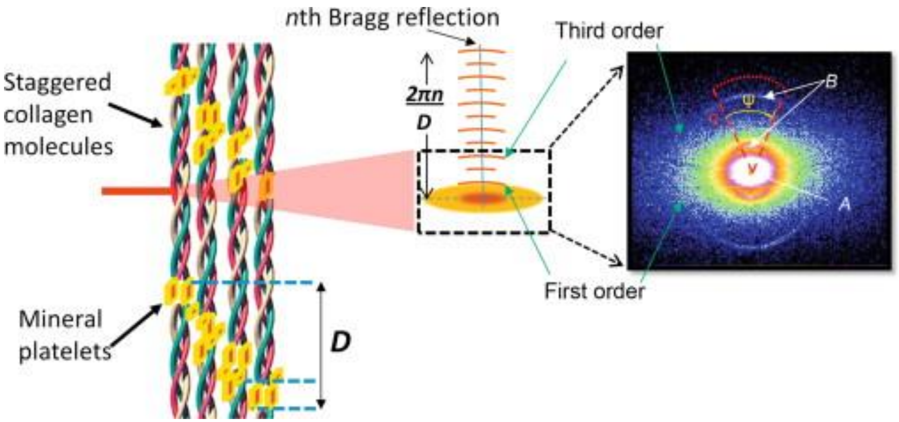

Karunaratne *et al.*, Methods in Enzymology, **532**, 2013, Pages 415–473

Carbon nanotube - 1-

The research group has a process to produce kilometres of continous macroscopic fibres of CNTs

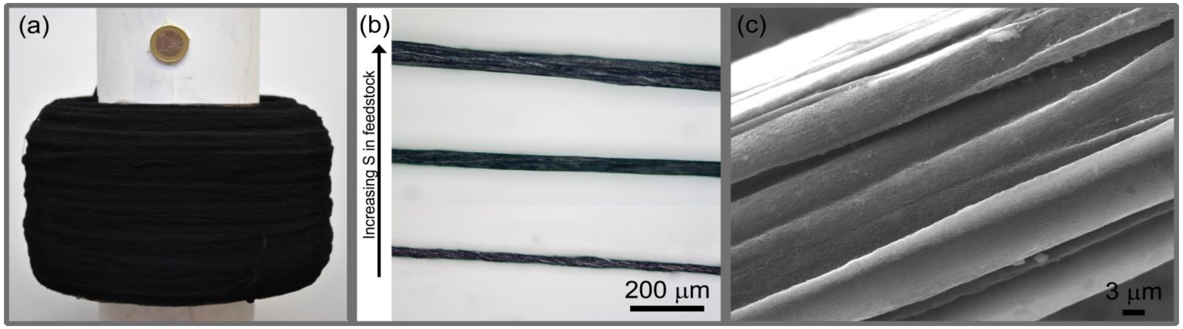

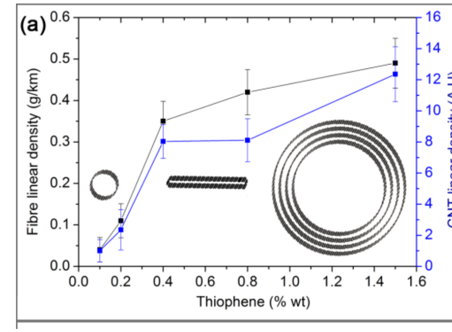

Synchrotron XRD confirms the increase of graphitic layers at turbostratic separation

S ↑ in feedstock → Intensity ratio [(100)Graphite / (111)Fe]

They can tailor thee type of nanotubes through the addition of sulphur precursor (thipohene)

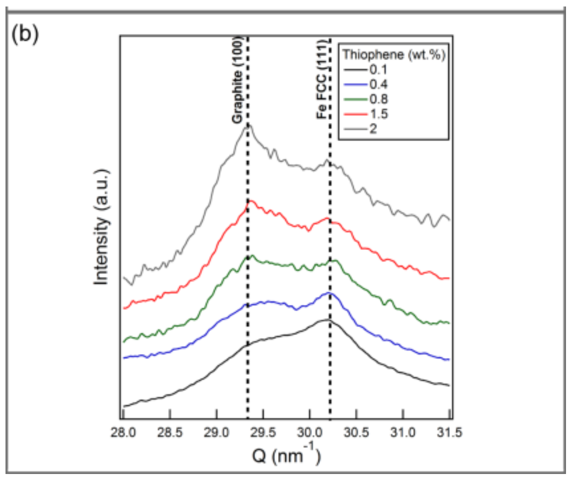

Low S → SWCNTs

High S → MWCNTs

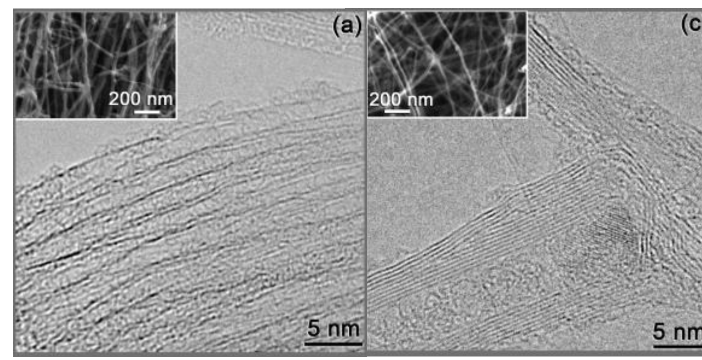

Reguero *et al.*, Controlling carbon nanotube type in macroscopic fibers synthesized by the direct spinning process , 2014, Chemistry of Materials, **26 (11)**, 3550-3557 DOI: 10.1021/cm501187x

Carbon nanotube - 2-

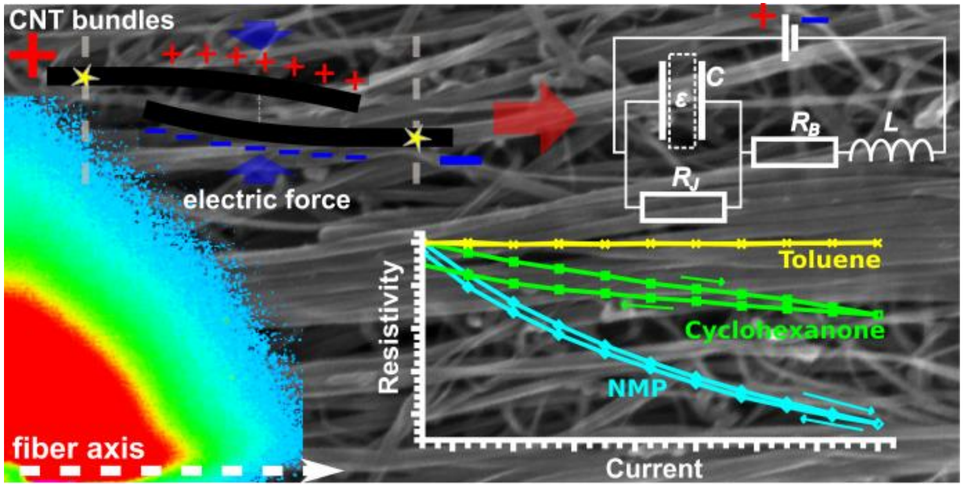

The CNT fibres have a complex hierarchical structure. Its mesoporosity makes liquids infiltrate the fibre, which changes its eletrical conductivity.

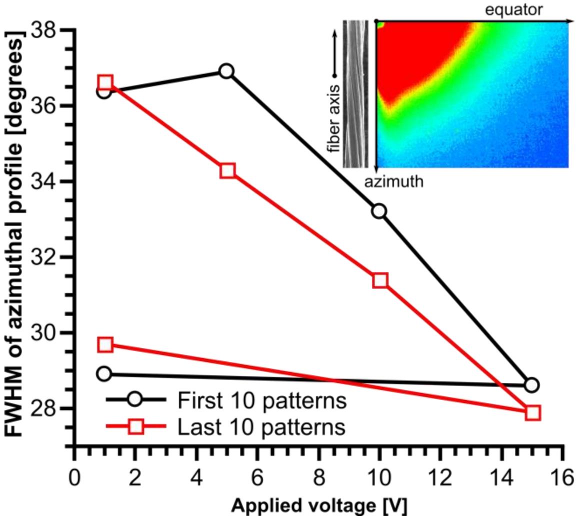

This non-Ohmic behaviour is a manifestation of nanoscale effects observed on a macroscopic scale.
It arises due to fibre swelling, which can be observed by SAXS.

Terrones *et al.*, Electric Field-Modulated Non-ohmic Behavior of Carbon Nanotube Fibers in Polar Liquids, 2014, ACS NANO, **8 (8)** , 8497-8504, DOI: 10.1021/nn5030835

Membrane vesicles - 1 -

From scattering theory, analytic expressions are derived for the bilayer form factor over a spherical geometry, assuming the lipid bilayer electron density to be composed of a series of Gaussian shells.

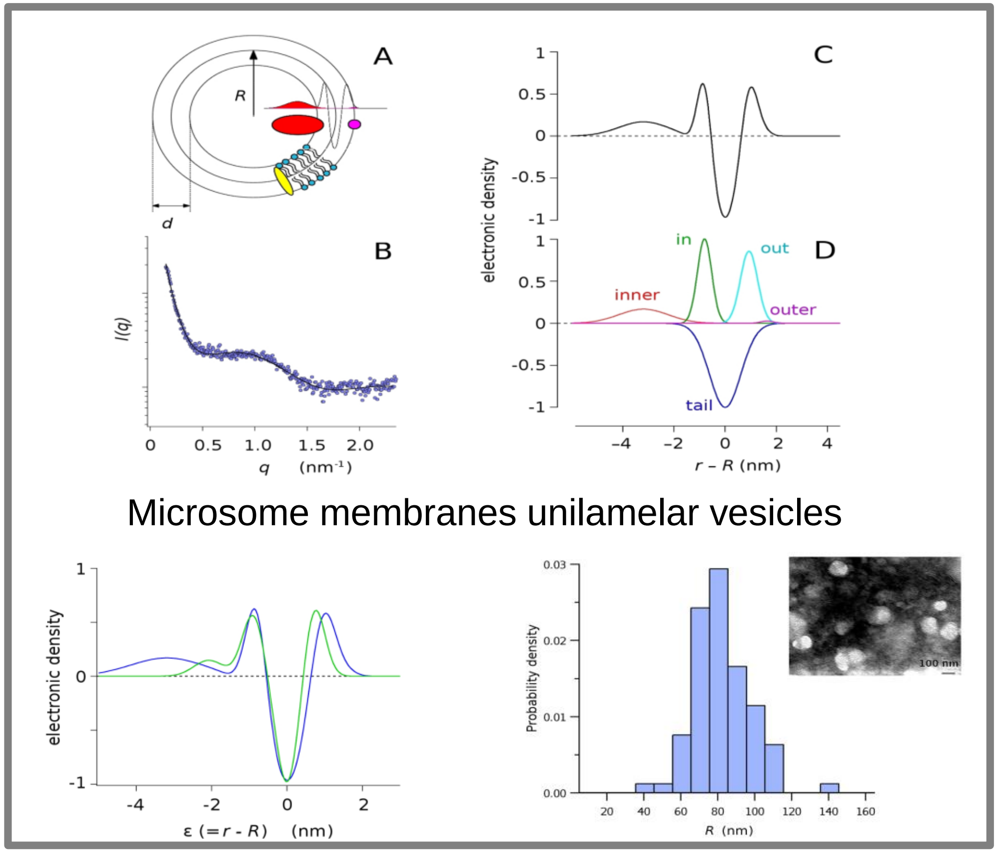

A) Sketch of the model of a vesicle consistent with the measured SAXS data.
B) SAXS spectra of the WT-CFTR membranes
C) The electronic density profile was calculated from the five Gaussian model
D) The decomposition of each singular Gaussian used to model the electronic density

Electron density profiles of from microsome vesicles wall of native cells (green) and cells overexpressing CFTR (blue; protein involved in cystic fibrosis). Micrographs of vesicles are shown.

Baroni et al., Direct interaction of a CFTR potentiator and a CFTR corrector with phospholipid bilayers, European Biophysics Journal, July 2014, Volume 43, Issue 6-7, pp 341-346

Membrane vesicles - 2 -

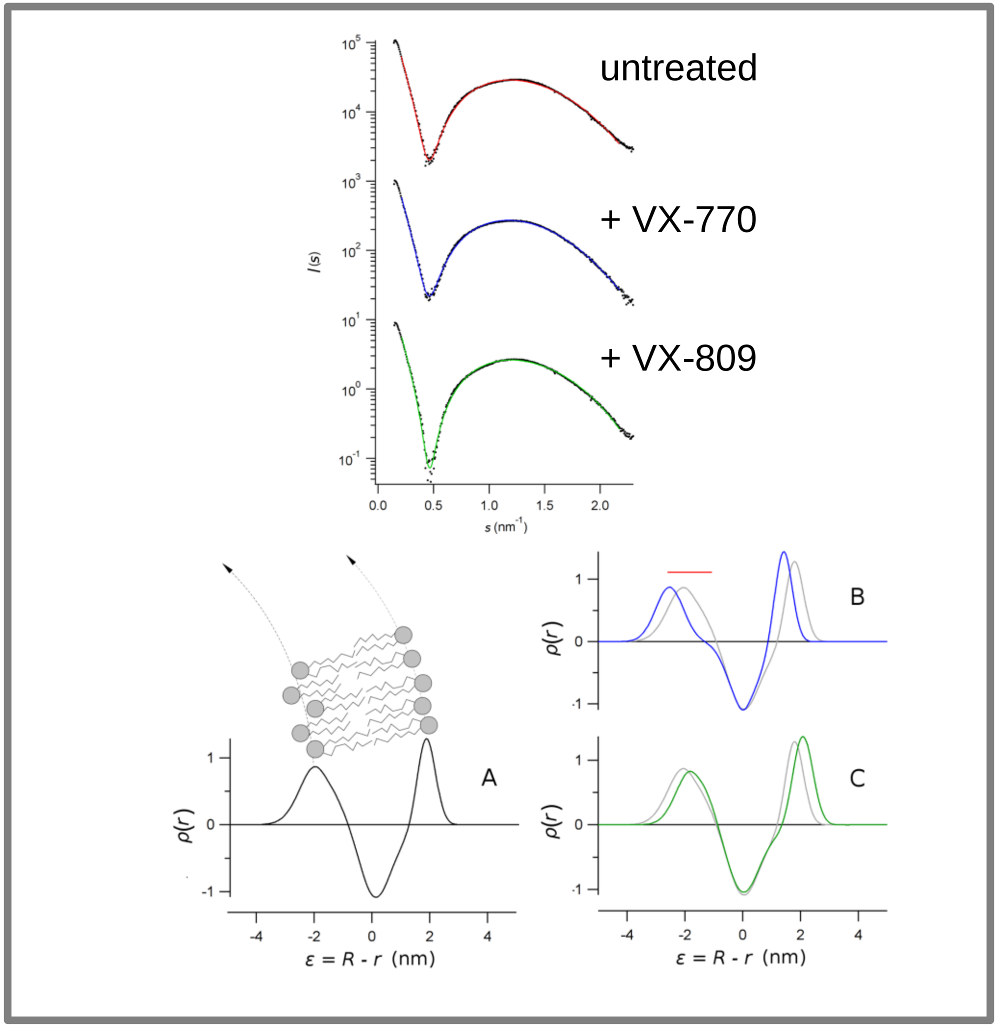

Large unilamellar liposomes (LUV) obtained by extrusion of phospholipids, treated with drugs for the cystic fibrosis therapy.

Electron density of the LUVs wall showing the destabilization induced by drugs.

Partially supported by the Italian Cystic Fibriosis Foundation

Particle in solution - 1 -

$$I(q) = \int_{V_r} \int_{V_{r'}} \Delta\rho(r)\Delta\rho(r')e^{-i\vec{q}(\vec{r}-\vec{r}')} dV_r dV_{r'}$$

$$p(r) = \frac{1}{(2\pi)^2} \int_0^\infty I(q) qr \sin(qr) dq$$

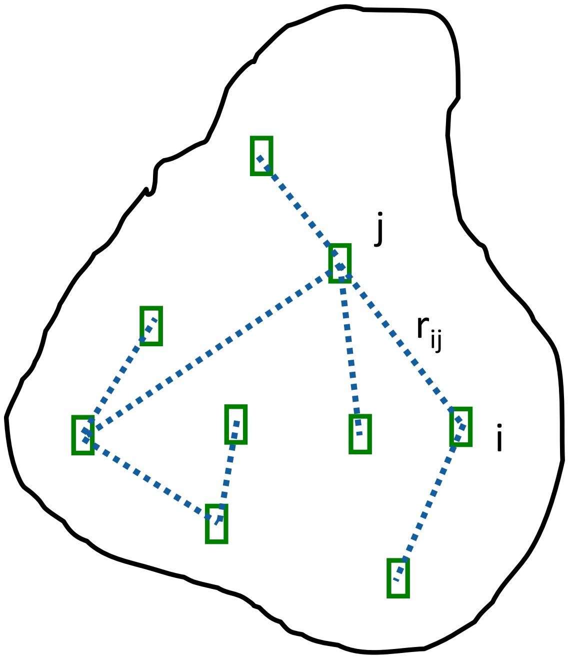

Probability of finding a point at r from a given point.

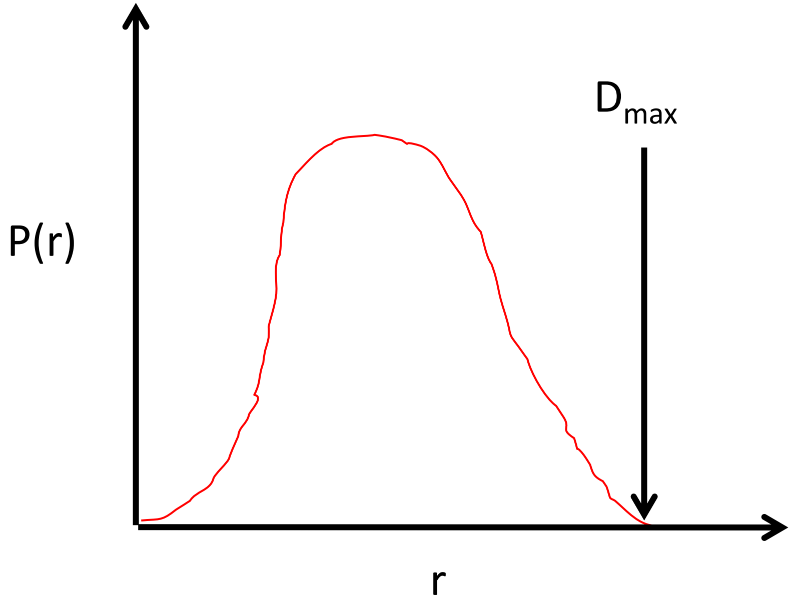

Particle in solution - 2 -

$$p(r) = \frac{1}{(2\pi)^2} \int_0^\infty I(q) qr \sin(qr) dq$$

In theory, very easy calculation

Problem:

The intensity :

- ✓ only known over q_{min}-q_{max} (Detector size)
- ✓ affected by experimental errors

$\Rightarrow$ Fourier transform of incomplete and noisy data is a ill-posed problem

Solution: Indirect Fourier Transform

Particle in solution - 3 -

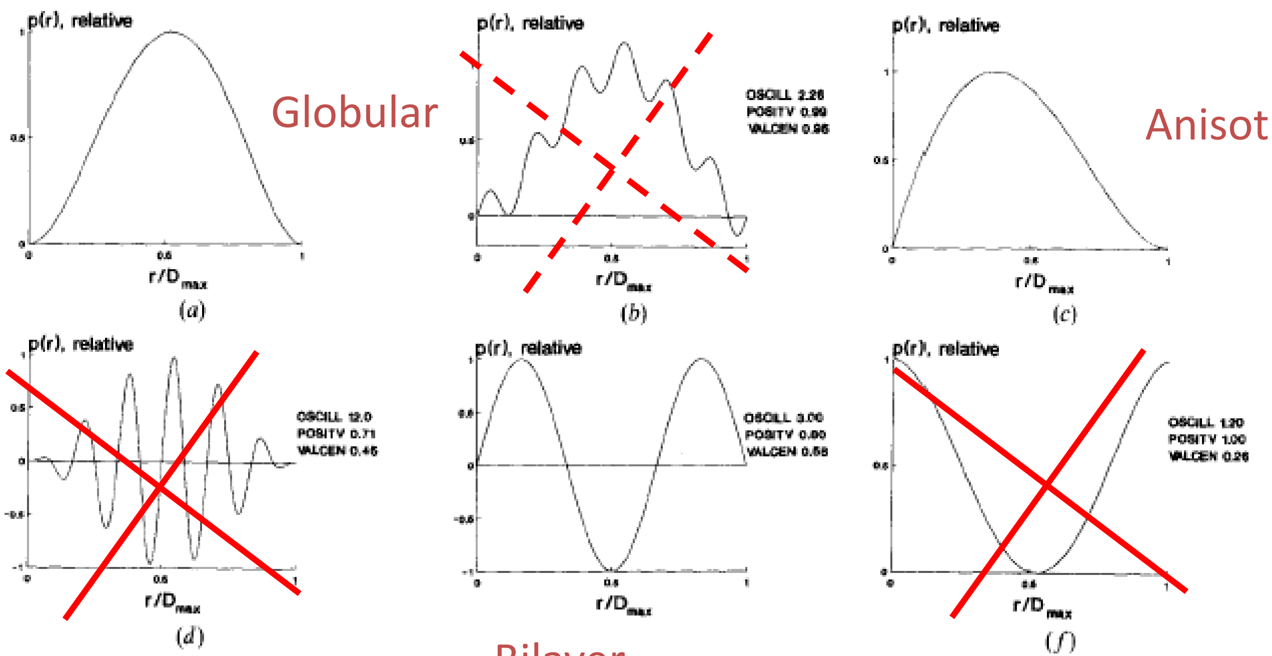

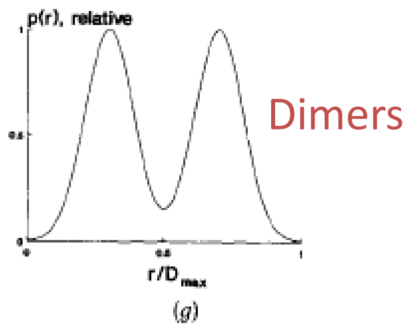

J. Appl. Cryst. (1992). **25**, 495–503

Determination of the Regularization Parameter in Indirect-Transform Methods Using Perceptual Criteria

By D. I. Svergun*†

GKSS Research Center, GKSS-WS, 2054 Geesthacht, Germany

Particle in solution - 4 -

Guinier Law

$$I(q) = 4\pi \int_0^\infty p(r) \frac{\sin(qr)}{qr} dr$$

Taylor series expansion of $\frac{\sin(qr)}{qr} = 1 - \frac{(qr)^2}{3!} + \frac{(qr)^4}{5!} - \ldots$

$$I(q) = \underbrace{4\pi \int_0^\infty p(r) dr}_{I(0)} \left[1 - \left(\frac{q^2}{3!}\right) \underbrace{\frac{\int_0^\infty r^2 p(r) dr}{\int_0^\infty p(r) dr}}_{2R_g^2} \right] = I(0) \left[1 - \frac{q^2 R_g^2}{3} \right]$$

Taylor series expansion of $e^x = 1 + x + \frac{x^2}{2!} + \frac{x^3}{3!}$ $\quad with \quad x = -\frac{q^2 R_g^2}{3}$

$qR_g \ll 1$

$$\boxed{I(q) = I(0) e^{-\frac{q^2 R_g^2}{3}}}$$

Particle in solution - 5 -

Accuracy of the Guinier Law

Valide for $qR_g << 1$

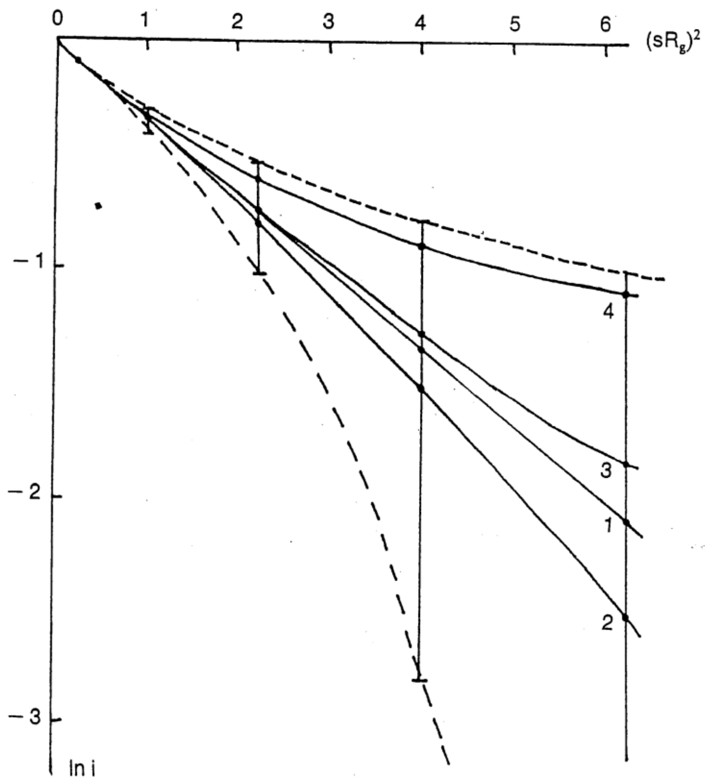

1 – Guinier law (exponential)

2 – Sphere

3 – Thin disk

4 – long rod

Depends on the shape of the particle

qR_g=1.5 about 20.0% – 30.0% error

qR_g<1.3 to reduce errors

Structure Analysis by Small Angle X-ray and Neutron Scattering
L.A. Feigin and D.I. Svergun (1987), Plenum Press.

Particle in solution - 6 -

Radius of gyration

$$R_g^2 = \frac{\int_{V_r} \Delta\rho(r) r^2 dV_r}{\int_{V_r} \Delta\rho(r) dV_r}$$

R_g is the quadratic mean of distances to the centre of mass weighted by the contrast of electron density

Rg is an index of non sphericity

Sphere: $Rg = \sqrt{\frac{3}{5}}R$

Smallest R_g for a given volume

Cylinder (D,H) $R_g = \sqrt{\frac{D^2}{8} + \frac{H^2}{12}}$

Ellipsoid of revolution (a,b) $R_g = \sqrt{\frac{2a^2 + b^2}{5}}$

Particle in solution - 7 -

Guinier Plot

$$I(q) = I(0)e^{-\frac{q^2 R_g^2}{3}}$$

$$\ln I(q) = \ln I(0) - \frac{q^2 R_g^2}{3}$$

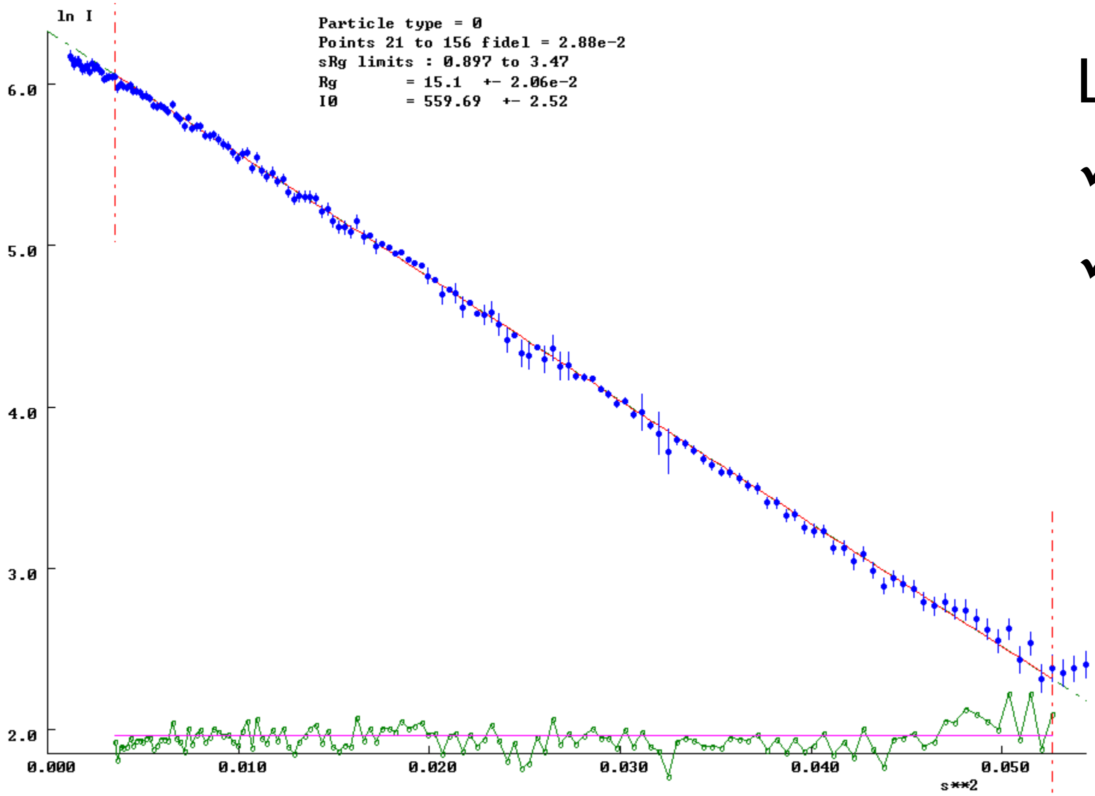

Linear regression

- ✓ Slope -> Rg^2
- ✓ Intercept -> I(0)

  -> M_w

Particle in solution - 8 -

Peak position = Zinc position

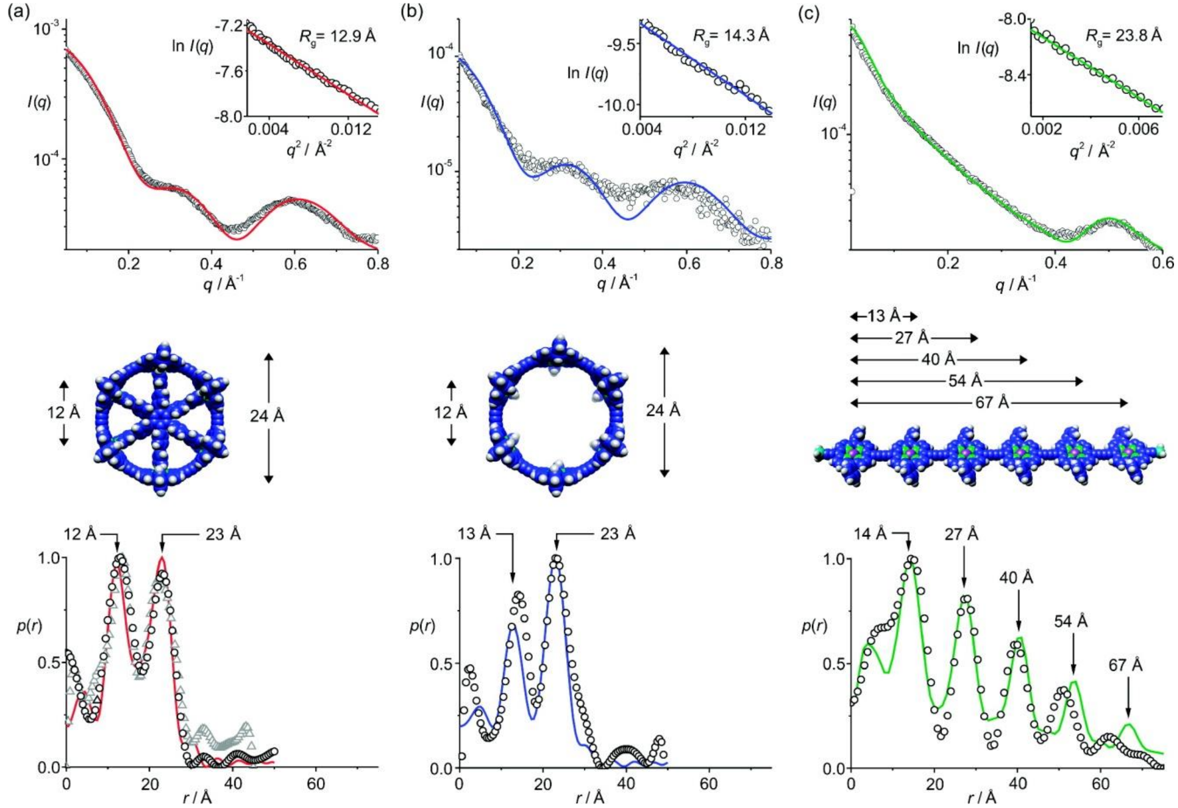

O'Sullivan *et al.*, Vernier templating and synthesis of a 12-porphyrin nano-ring, Nature, (2011) 469, 72–75

Beamline staff

Beamline Responsible:
  Marc Malfois
Beamline scientist:
  Christina Kamma-Lorger
  Juan-Carlos Martinez
Postdoctoral Research Associate:
  Eva Crosas
Technician:
  Jordi Prat
Controls:
  Gabriel Jover
Engineering:
  Joaquin Gonzalez
  Carles Colldelram
Electronics:
  Abel Fontsere